OATAO
Open Archive Toulouse Archive Ouverte

Open Archive Toulouse Archive Ouverte (OATAO)

OATAO is an open access repository that collects the work of Toulouse researchers and makes it freely available over the web where possible

This is an author's version published in: **http://oatao.univ-toulouse.fr/19791**

Functionalized superhydrophobic coatings with micro-/nanostructured ZnO particles in a sol–gel matrix

Q. Boyer[1] , S. Duluard[1] , C. Tenailleau[1,*] , F. Ansart[1] , V. Turq[1] , and J. P. Bonino[1]

[1] CIRIMAT, Université de Toulouse, CNRS, INPT, UPS, Université Toulouse 3 Paul Sabatier, 118 route de Narbonne, 31062 Toulouse Cedex 9, France

ABSTRACT

Among the methods to create superhydrophobic surfaces by wet chemistry, one of the strategies consists in coating the substrate with a hydrophobic polymer with specific morphology. Such elaborated surfaces are largely developed and can present complex architectures but are generally fragile. Ceramic-based coatings show better durability. In this work, a new route associating inorganic and polymeric parts is used. Surfaces with superhydrophobic properties are prepared with a mixture of zinc oxide (ZnO) particles in a hybrid organic inorganic matrix prepared via sol–gel route. ZnO particles were synthesized by the inorganic polycondensation route and exhibit an appropriate micro-/nanostructure for superhydrophobicity. Sol–gel matrix is obtained by the alkoxide route with aluminum-tri-sec-butoxide (ASB) and (3-glycidoxypropyl)trimethoxysilane (GPTMS). A step of octadecylphosphonic acid (ODP) functionalization on ZnO particles and on film surfaces was employed to considerably improve hydrophobic properties. This new route enables to obtain superhydrophobic coatings that exhibit water contact angles superior to 150°. These coatings show a homogeneous and smooth coverage on aluminum alloy substrate. Results attest the significance of the synergy for superhydrophobic coatings: a micro-/nanostructured surface and an intrinsic hydrophobic property of the material. The durability of the coatings has also been demonstrated with only a slight decrease in hydrophobicity after erosion.

Introduction

Wettability of a surface is governed by its chemical properties and microstructure and is defined by the aptitude of a liquid drop to spread over the solid surface. Interest for superhydrophobic surfaces (usually defined as having a water contact angle (CA) over 150°) is wide for various applications including self-cleaning materials (glass, textile, paints) or non-adhesive surface for microfluidics for drag reduction [1, 2]. For such applications, non-adherent

superhydrophobic surfaces are preferred, i.e., in a Cassie–Baxter's superhydrophobic state [3]. This behavior is obtained when the micro-/nanostructured material is itself hydrophobic [4]. It has been showed that the increase in specific area and consequently the roughness lead to a better superhydrophobic property [5].

Zinc oxide (ZnO) is a material of choice to prepare particles with multiscale structuration from micrometer to nanometer sizes [5–7]. Morphology-controlled ZnO nanoparticles preparation methods involve hydrothermal synthesis [7, 8], low-temperature precipitation [6, 9, 10], chemical vapor growth [11], sputtering [12], electrophoretic deposition [13] and sol–gel [14] methods. A large list about superhydrophobic surfaces preparation has been recently proposed by Zhang et al. in their review [15]. Some examples of superhydrophobic architectures using ZnO and/or others materials are given in Table 1. A micro-/nanostructured ZnO film with contact angle as high as 161° has been obtained with pure ZnO (cf. Table 1 line A) as it is intrinsically hydrophobic as long as the strict stoichiometry is followed [14]. However, to guarantee the properties for longer lifetime, it is generally preferred to coat the structured surfaces with a hydrophobic coating. Polydimethylsiloxane (PDMS), polytetrafluoroethylene (PTFE or Teflon), octadecyltrimethoxysilane (OTMS), octadecylphosphonic acid (ODP) or stearic acid (AC) are the most usual materials to confer hydrophobic properties to the coating. Therefore, many works were dedicated to the development of micro-/nanostructured films and to their surface functionalization with hydrophobic materials (cf. table 1 line B). Some authors have elaborated superhydrophobic coatings with hydrophobically functionalized particles in the matrix (cf. table I line C). The main purpose is to extend the superhydrophobic behavior through all the samples.

In this paper, the three different ways to get superhydrophobic coatings have been combined: micro- and nanostructured films have been prepared including hydrophobically functionalized ZnO particles with an organic compound. Superhydrophobic film properties were compared with coatings without particles functionalization and with/or without film functionalization.

The four-step protocol has been set up as follows. First, ZnO micro-/nanoparticles were synthesized by inorganic polycondensation based on works of Salek et al. [9] or Sun et al. [10] using two types of alkaline solutions. The influence of the alkaline solution nature is related to the ionic radius of the element $(r(Li^+) = 0,73$ Å and $r(Na^+) = 0,97$ Å). Li^+ benefits from smaller ionic radius than Na^+ (for the same elementary charge) so that the positive surface charge is higher for particles prepared with Li^+, charge repulsion increases, and subsequent particles growth is inhibited [16–18] so that different micro- and nanostructures can be obtained. After functionalization with hydrophobic octadecylphosphonic acid (ODP), ZnO particles have been dispersed in an alcoholic solution including a dispersing agent (polyvinylpyrrolidone) and a metal alkoxide-based sol. A slurry is obtained and deposited by dip coating on the aluminum substrates. After sol–gel transition and thermal treatment,

Table 1 Various superhydrophobic architectures: examples of some superhydrophobic architectures in the literature with information about materials and water contact angle property

Architecture		Materials	Water CA	References
A	Hydrophobic micro-/nanostructured materials	ZnO	151°	[7]
		ZnO	161°	[14]
B	Hydrophobic layer on a microstructure	ZnO with Teflon-AF	168°	[8]
		ZnO with stearic acid	175°	[26]
		Acrylic polymer and silica with silane	152°	[27]
		TiO_2 with PTES	157°	[28]
C	Hydrophobic particles in a matrix	SiO_2, ZnO and ITO in silicone resin	169°	[22]
		PFOS/POTS in polymer complex	165°	[29]
		$CaCO_3$ in PDMS	153°	[30]

a structured coating of ZnO particles emerging from a matrix is obtained. An additional step of surface functionalization with ODP has been employed. The morphology of particles and films depending on the synthesis parameters is discussed as well as the wettability of the films and their durability.

Materials and methods

Raw materials

The substrate is an aluminum alloy rich in silicon and magnesium AS7G06 from 2.0×2.7 cm size often used in aeronautics field. Zinc nitrate hexahydrate 98% $Zn(NO_3)_2$-$6H_2O$, sodium hydroxide $\geq$98% (NaOH), lithium hydroxide $\geq$98% (LiOH), 1-propanol 99.7% ($CH_3(CH_2CH_2OH)$, 2-propanol 99.8% (($CH_3)_2CHOH$), heptane 99% ($CH_3(CH_2)_5CH_3$), nitric acid 65% (HNO_3), aluminum-*tri-sec*-butoxide 97% (ASB), (3-glycidoxypropyl)trimethoxysilane $\geq$98% (GPTMS) and octadecylphosphonic acid 97% (ODP) were purchased from Sigma-Aldrich. Polyvinylpyrrolidone K12 (M.W. 3500 g/mol) was purchased from Acros Organics. The chemicals were used as received.

Shaping step

The diagram for particles and coatings preparation is given in Fig. 1 and described below.

ZnO particles were synthesized by inorganic polycondensation by using two different protocols described in the literature [10, 11]. The adapted protocol consists in dissolving 0.006 mol of $Zn(NO_3)_2$-$6H_2O$ in 120 mL of pure distilled water; then, 0.3 mol of NaOH or LiOH was added to the solution. After stirring for 2 h at room temperature, the final white precipitate was washed with deionized water and anhydrous ethanol in order to remove residual ions (OH^-, Li^+ and NO_3^-). It was then separated by centrifugation (twice) and dried at 80 °C for 13 h. The particles obtained from NaOH were called ZnO-Na, and those from LiOH were called ZnO-Li.

The formulation of the sol is based on the alkoxide route [19–21]. 0.027 mol of aluminum-*tri-sec*-butoxide (ASB) was diluted in 1.22 mL 1-propanol. Then, the solution was mixed with 0.063 mol (13.9 mL) of (3-glycidoxypropyl)trimethoxysilane. Finally, 13.43 mL of acidified water (with HNO_3 65%) was added. All the components were mixed with a 100 tr/min agitation, and the final mixture was kept to maturation during 24 h.

Figure 1 Diagram of particles and coatings (in *gray*) preparation. Hydrophobic materials are represented in *green* color.
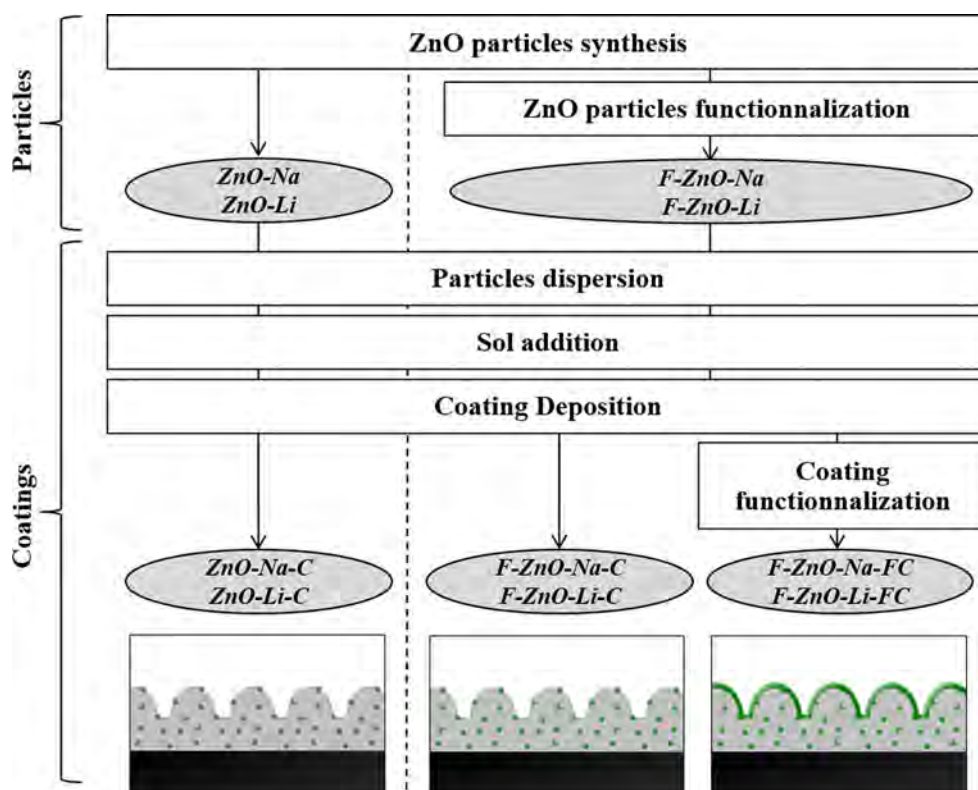
0.5 g of synthesized particles (ZnO-Na and ZnO-Li) was dispersed in 4 mL of a 1wt.% polyvinylpyrrolidone solution in 1-propanol. The dispersion was mixed with 0.5 g of sol solution. The substrate was washed in acetone with sonication before coating. Finally, the coating was prepared by dip coating using a Nadetech Dip-Coater with a withdrawal rate of 250 mm/min. The sample was dried at 110 °C for 4 h. Coatings were named ZnO-Na-C and ZnO-Li-C for coatings with ZnO-Na and ZnO-Li particles, respectively.

Two types of functionalization were used in this work. Particles functionalization was used with the addition of 2 g ZnO particles in 100 mL of a 2 mM ODP solution in ethanol for 96 h at 25 °C. Particles were dried at 110 °C for 1 h to improve ODP-ZnO bonds [22]. On the other hand, coating functionalization was used that consist in the immersion of the sample during 48 h at 25 °C in a stirred 5 mM ODP solution in a heptane/2-propanol (1000:7 v/v) mixture [23]. An additional step of 2-propanol rinsing was performed before drying at 110 °C for 4 h. F-ZnO-Na-C and F-ZnO-Li-C are, respectively, ZnO-Na-C and ZnO-Li-C particles functionalized coatings, whereas F-ZnO-Na-FC and F-ZnO-Li-FC are, respectively, ZnO-Na-C and ZnO-Li-C surface and particles functionalized coatings.

Characterization methods

X-ray diffraction (XRD) patterns were recorded on a Bruker D4-Endeavor instrument (40 kV, 40 mA) with a CuKα wavelength, from 10 to 100° in 2-theta, step size of 0.02° and 3.6 s/step scan. ZnO particles were characterized by field emission gun–scanning electron microscopy (FEG-SEM) on a JEOL JSM 6700F instrument, and coatings were characterized on a JEOL JSM 6400 instrument (SEM). Contact angle measurements were performed with a GVX DGD-FAST/60 goniometer and the WinDrop + software. Water droplets are 4 μL in volume, and measurements were taken 30 ms after deposition. Micromeritics FlowSorb II 2300 was used to determine the surface area of ZnO particles using a nitrogen 30 vol.% in helium mixture. Before calculating the specific surface area, the sample was degassed under nitrogen at room temperature for

1 h. Attenuated total reflectance infrared (ATR-IR) analyses were performed on a Thermo Nicolet Nexus 670 FTIR instrument. Surface topology was obtained by a Sensofar Sneaox confocal microscope with green light. The microstructure was observed with a Nanoscope III Dimension 3000 Atomic Force Microscope (AFM). Durability tests were carried out with glass marbles from 245 to 450 μm in diameter during 10 s. The gun was placed at 30 cm from the sample with an incidence angle of 90° and 3 bars pressure.

Results and discussion

ZnO particles characterization

XRD patterns of ZnO-Na and ZnO-Li particles are plotted in Fig. 2. For each sample, all peaks are indexed with a hexagonal structure of zinc oxide (JCPDS 01-070-8070). This indicates the presence of crystalline ZnO with high purity (>95%). Williamson–Hall method [24, 25] reveals that the preferred growth orientation is along the c-axis for both samples. Crystallite size along the c-axis is 141 nm for ZnO-Na and 143 nm for ZnO-Li whereas around 50–60 nm along other directions for both particles. ZnO-Na and ZnO-Li smaller crystallites are very similar.

On the contrary, the shape of the ZnO particles is largely depending on the alkaline solution used for the synthesis. FEG-SEM images of ZnO particles (Fig. 3) reveal that ZnO-Na particles are sandrose-shaped (Fig. 3a, b) and ZnO-Li particles have a urchin-like structure (Fig. 3c, d). In both cases, these microsized structures are formed from agglomeration of nanosized particles (nanoplates of 17 ± 3 nm in thickness and approximate size for flakes of 3 ± 1 μm and nanospikes of around 150 nm size for flowers of 1–2 μm size with 10 μm agglomerates). This evidenced a two-level structuration (micro and nano) of these particles which is expected to be beneficial for the preparation of superhydrophobic coatings.

Furthermore, LiOH leads to smaller particles than NaOH in accordance with their cationic radii [17]. The morphology of these particles is homogeneous and reproducible. The specific surface area is similar for ZnO-Na and ZnO-Li particles with 17.4 and 15.5 m^2/g, respectively.

Figure 2 XRD patterns of ZnO-Na *a* and ZnO-Li *b* particle and indexing JCPS 01-070-8070 of zinc oxide *c*.
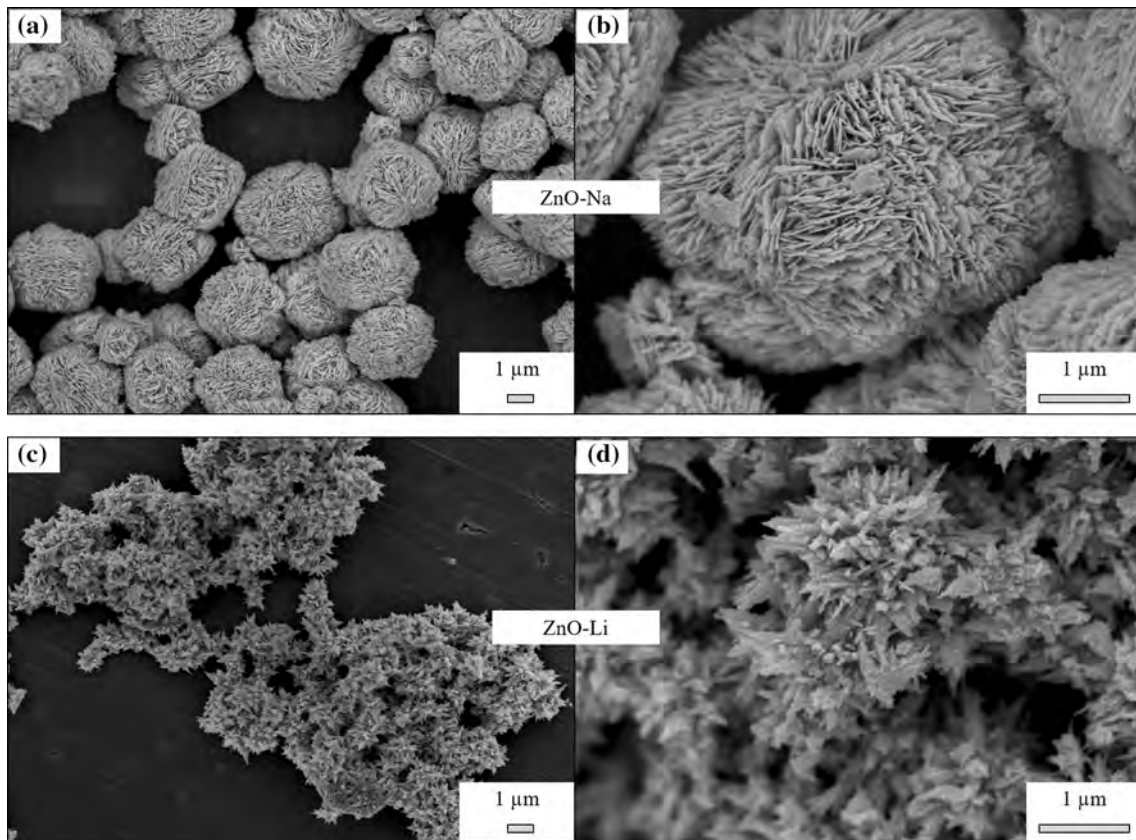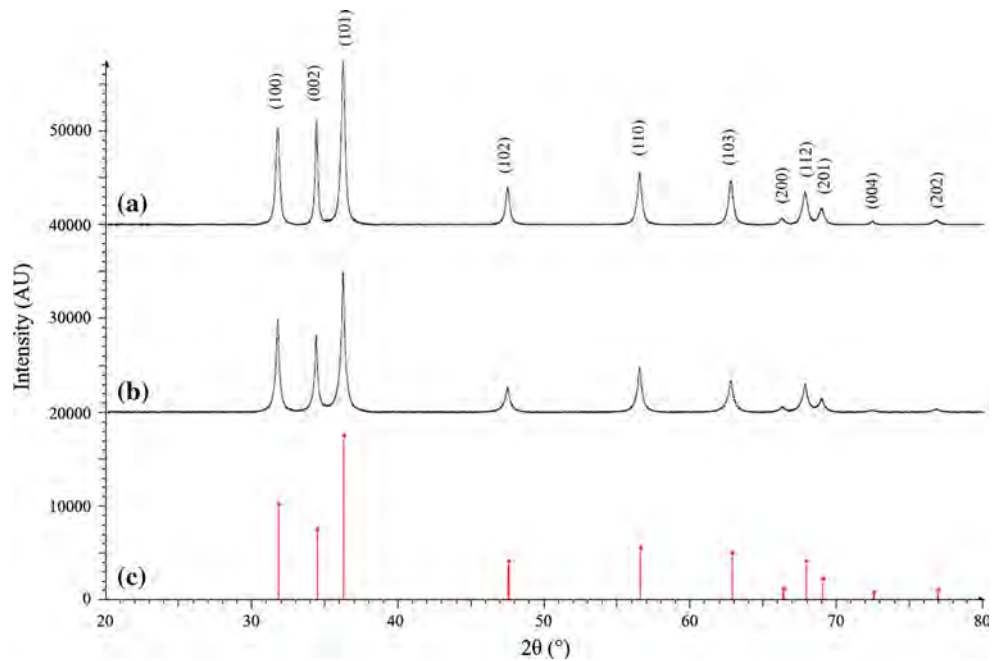
Figure 3 FEG-SEM images of ZnO-Na particles **a** and **b** and ZnO-Li particles **c** and d.

Film morphology

Surface coverage

SEM images of ZnO-Na-C coating and ZnO-Li-C coating are shown in Fig. 4a–d. ZnO-Na-C has a smaller coverage area than ZnO-Li-C (5% for ZnO-Na-C and 31% for ZnO-Li-C). This difference is possibly due to larger size ZnO-Na particles that cannot be carried by the sol solution on the substrate. This might result in ZnO particles sedimentation at the bottom of the dip-coating cell and a small amount of ZnO-Na particles in the ZnO-Na-C coating. Nevertheless, there is a homogeneous coating all over the surface area (Fig. 4a, c). Two other types of coatings were elaborated with ODP-functionalized ZnO particles. Resulting FEG-SEM images of the second type of coating (F-ZnO-Na-FC and F-ZnO-Li-FC) are presented in Fig. 4e–h. The latter is composed of ODP-functionalized ZnO particles and ODP-functionalized coating surfaces. It is obvious that ODP functionalization particles significantly improve the coverage area (100% for F-ZnO-Li-FC and 43% for F-ZnO-Na-FC) (Fig. 4e, g). It is likely that the ODP functionalization acts as a very good ZnO particles dispersing agent in the coating solution in combination with PVP even if the sol solution is aqueous. On the other hand, PVP alone may not impact the ZnO particles dispersion. Regarding the surface functionalization, it is considered that ODP grafting does not affect the coating homogeneity according to the only top coating surface alkyl groups grafting. So it is supposed that functionalized ZnO particles coatings and functionalized ZnO particles and surface coatings have the same microstructure and coverage area. Moreover, a smoothing phenomenon of the coating surface after ODP functionalization can be noticed (Fig. 4f, h).

Surface chemistry and topology

The presence of ODP at the surface of the coatings has been verified by ATR-IR analyses. The ATR-IR spectrum revealed absorption peaks at 2848 and 2916 cm^{-1} due to –CH$_2$-stretching vibrations. Another peak at 1463 cm^{-1} attests the presence of C–H bending vibrations. There results attest to the effectiveness of the ODP grafting.

Surface topology analyses were performed by confocal microscopy (Fig. 5). As also observed by SEM, the surface coverage for the coating prepared with Na-based particles (F-ZnO-Na-FC) is not ideal, with lamination ridges still visible, whereas a full coverage is obtained for the Li-based particles (F-ZnO-Li-FC).

Wettability

The superhydrophobic property of each coating was estimated by measuring the water contact angle (CA) of the coated surface. For comparison purpose, the same measurements were done on the substrate itself and the sol–gel matrix deposited on the substrate. Substrate and sol–gel matrix are hydrophilic with a water CA of $83 \pm 2°$ and $69 \pm 1°$, respectively (Fig. 6). CA values increase as ODP functionalization surface is performed ($115 \pm 2°$ for the functionalized substrate and $89 \pm 2°$ for the functionalized sol–gel matrix). This result demonstrates that the sol–gel matrix is mostly hydrophilic, whereas ODP functionalization will play the major role in obtaining superhydrophobic coatings.

The CA measurements on ZnO coatings are presented in Fig. 7. The coatings from non-functionalized particles are not hydrophobic (CA = $74 \pm 2°$ and CA = $79 \pm 1°$ for ZnO-Na-C and ZnO-Li-C, respectively), which is due to the small covered area as shown by SEM images (Fig. 4a, c). On the contrary, coatings obtained from ZnO particles that were functionalized, the hydrophobic character of the coatings increases with CA of $98 \pm 1°$ and $111 \pm 3°$ for F-ZnO-Na-C and F-ZnO-Li-C, respectively. This increase in CA is largely due to a better surface coverage after ODP functionalization particles that stabilizes dispersion and is also due to the hydrophobic hydrocarbon tails of ODP.

Adding an ODP functionalization step after coating was necessary in order to obtain a strong superhydrophobic character. Such coatings present contact angles of 153° and 155° for F-ZnO-Na-FC and F-ZnO-Li-FC, respectively, as shown in Fig. 7. For both of them, the superhydrophobic property is related to the expected synergy previously established: an ODP functionalization that involves hydrophobic state with a ZnO-based homogeneous coating that insures a micro-/nanostructure with high coverage to reach a superhydrophobic state.
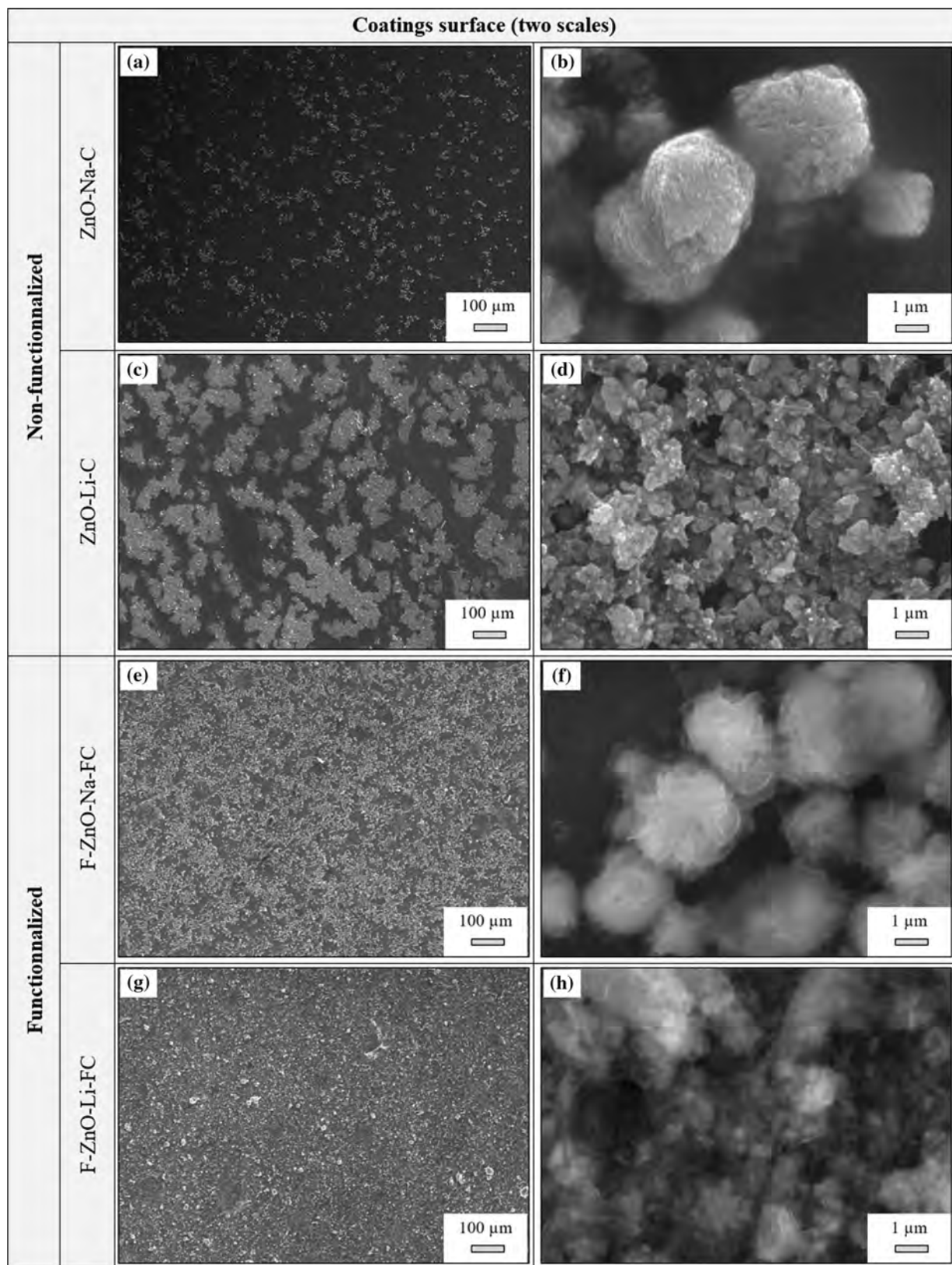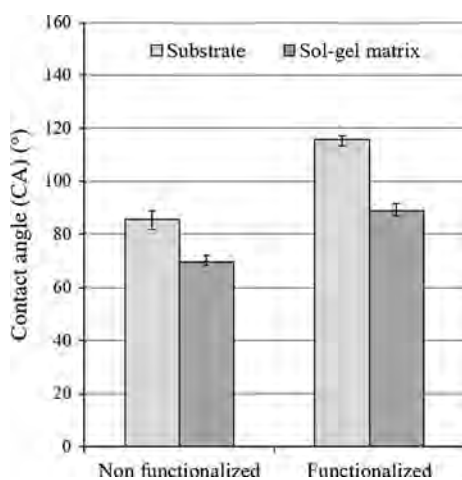
Figure 4 SEM images coatings: ZnO-Na-C **a** and **b**, ZnO-Li-C **c** and **d**, F-ZnO-Na-FC **e** and **f** and F-ZnO-Li-C **g** and **h**.
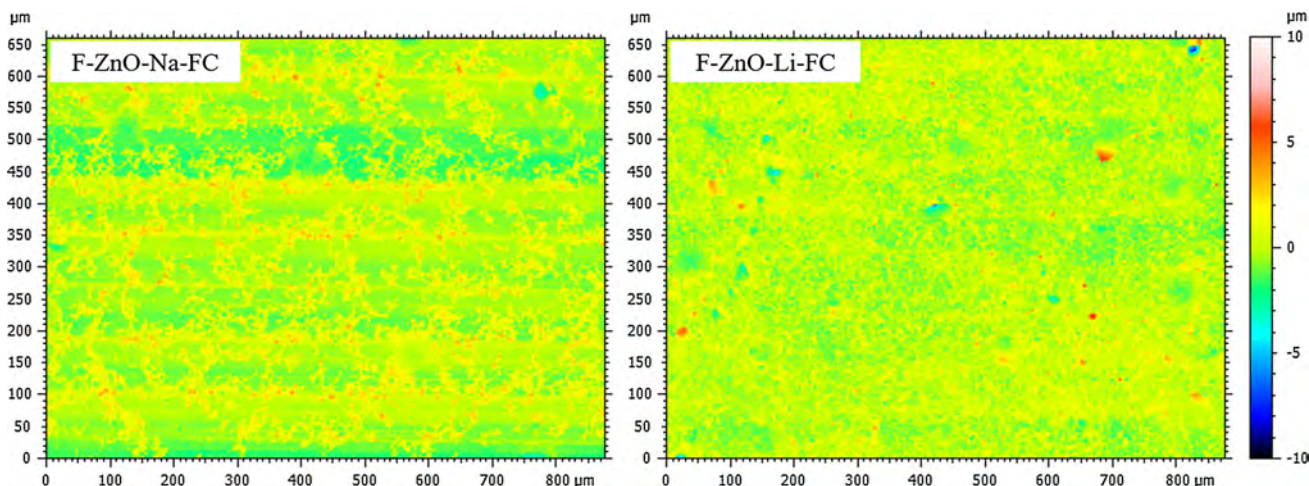
Figure 5 Topology of coatings: F-ZnO-Na-FC and F-ZnO-Li-FC.

Figure 6 Contact angles comparison of substrate and sol–gel matrix with and without functionalization.

Coatings performance after durability tests

### Surface topology and chemistry after durability tests

Figure 8 shows that the surface topology is affected by the erosion. Large craters are present at the surface of the coating, which size is consistent with the diameter of the sand used for erosion (250–400 µm). However, ODP remains at the surface of the coating, as analyzed by ATR-IR, with the presence of absorption peaks at 1463, 2848 and 2916 cm^{-1}. Moreover, EDS analyses attest the presence of zinc even in the places where the coating has been flattened by the sand beads (Fig. 9). In particular, the F-ZnO-Li-FC-E exhibits a Zn signal on the whole coating. The coating is present even at the bottom of the craters, which demonstrates the high cohesive properties of the coatings. The films are also highly adhesive: no delamination or cracks were observed after durability tests.

Coatings wettability after durability tests

Regarding wettability, coatings from ODP-functionalized ZnO particles followed by ODP functionalization surface present a CA of 127 ± 2° (vs. 153° before erosion) and 130 ± 2° (vs. 155° before erosion) for F-ZnO-Na-FC-E and F-ZnO-Li-FC-E coatings, respectively. The decrease in hydrophobicity after durability tests is limited (around 15%), and the contact angle remains superior to that of non-functionalized coatings (Fig. 7 F-ZnO-Na/Li-C). As already discussed, superhydrophobic properties are both due to the surface structuration at the micro- and nanoscales, as well as the surface chemistry (hydrophobic character of the material). IR analyses demonstrated the presence of hydrophobic species at the top of the coating, even after durability tests, but with a lower signal intensity. Regarding the micro-/nanostructure, microscale topological analyses indicate remaining microstructuration even after durability tests (Fig. 8).

**Figure 7** Contact angles measured for all coatings.
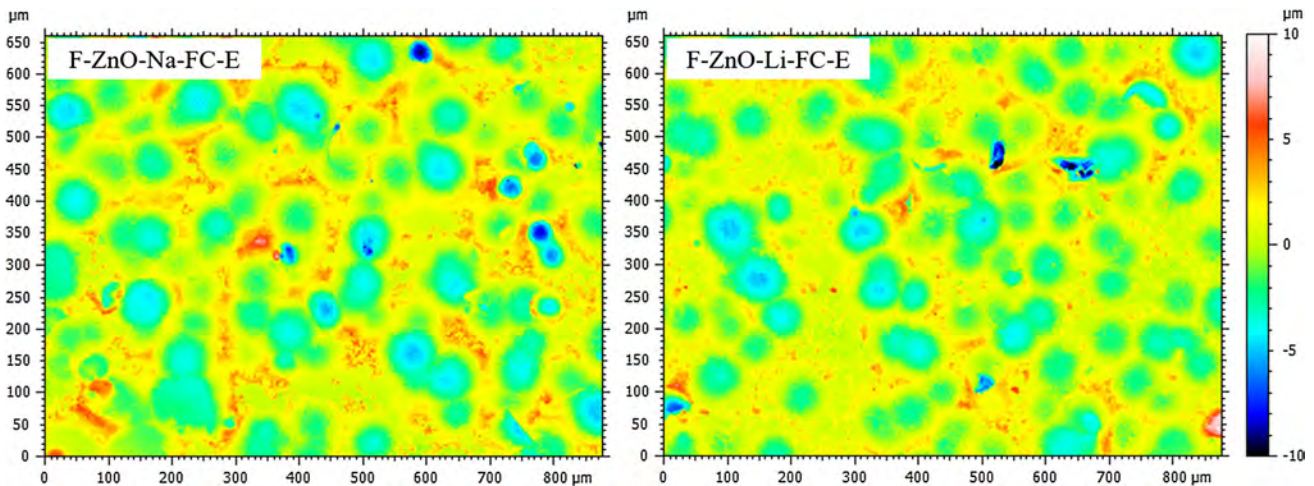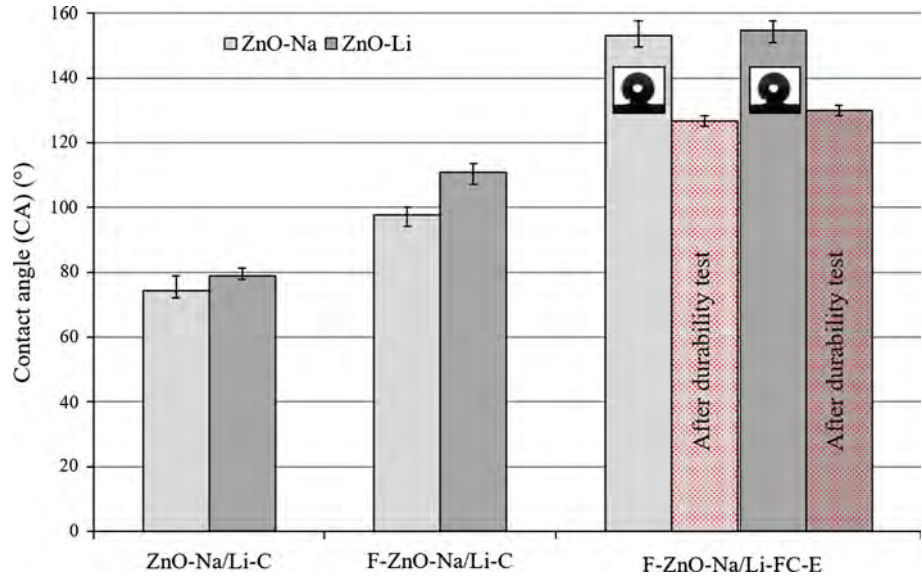
Figure 8 Topology of coatings after durability tests: F-ZnO-Na-FC-E and F-ZnO-Li-FC-E.
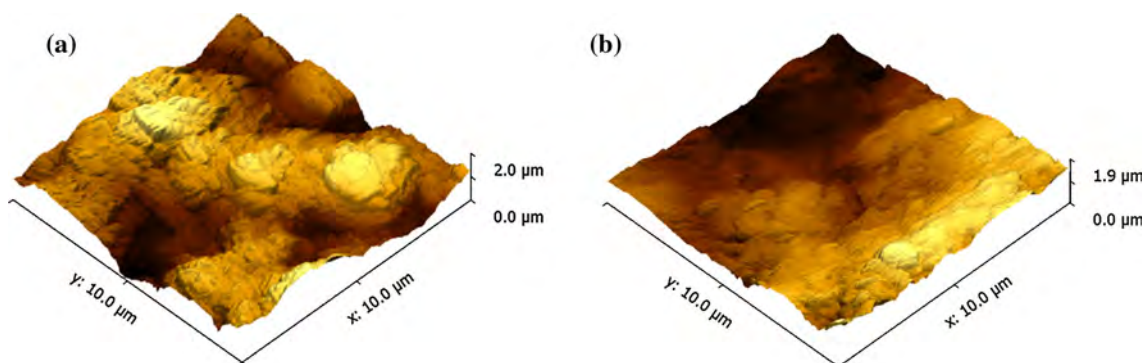
Nanostructuration of the coatings

AFM analyses performed on the most promising composition, F-ZnO-Li-FC, give a better insight on the nanoscale morphology of the coating before (Fig. 10a) and after durability tests (Fig. 10b). The same arithmetic mean roughness of 0.32 ± 0.01 μm is measured for the sample before and after durability tests. However, the shape of the roughness is different with a skewness changing from −0.22 to −0.03 and a kurtosis from −0.47 before to −0.85 after durability tests. Indeed, the overall roughness is similar with only a small impact of the durability tests: the predominance of holes before erosion is attenuated after erosion, but holes are stepper after erosion. Durability tests caused the removal of ODP functionalization parts, as well as the digging of microscale craters due to erosion beads, which revealed the nanoscale inner structuration of the coating. Then, the resulting surface benefits from both a micro- and a nanostructuration and the decrease in ODP functionalization thickness is partially compensated by this hydrophobic favorable morphology.
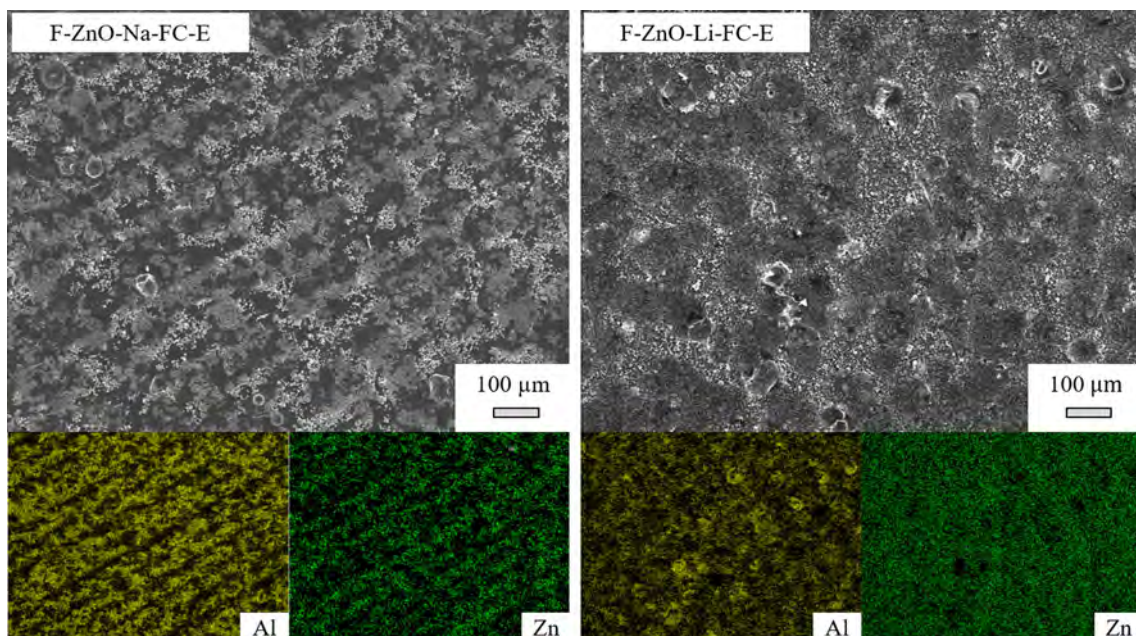
Figure 9 SEM images and EDS analyses of coatings after durability tests: F-ZnO-Na-FC-E and F-ZnO-Li-FC-E.

Figure 10 AFM images of the F-ZnO-Li-FC coating before **a** and after **b** durability tests.

Conclusions

ZnO coatings were prepared with ODP functionalization either only on the particles or on both particles and coatings. Micro-/nanostructures were obtained with ZnO particles synthesized via the inorganic polycondensation reaction. Particles with complex micro- and nanoscale morphologies were obtained. ZnO particles were immersed in a sol–gel matrix to get coatings with or without functionalization. Additional functionalization was also employed on the coating surface. Superhydrophobic coatings with a good homogeneity were obtained after ODP functionalization of particles and surface.

On one hand, it was shown that functionalization particles have a consequent influence on the coverage of coating to get the micro-/nanostructure expected. On the other hand, surface functionalization has a direct impact on the hydrophobic property of the coating. Furthermore, the high adherence and durability of the coatings have been demonstrated by erosion tests, with only a slight degradation of the water contact angle (15% decrease). In future works, it should be interesting to optimize ZnO particles coverage with thinner micro-/nanostructured particles or other dispersion protocols and coating depositions. Another way is to improve ZnO particles and sol–gel matrix chemical affinity by reformulation.

References

[1] Nosonovsky M, Bhushan B (2009) Superhydrophobic surfaces and emerging applications: non-adhesion, energy, green engineering. Curr Opin Colloid Interface Sci 14:270–280

[2] Bhushan B, Jung YC (2011) Natural and biomimetic artificial surfaces for superhydrophobicity, self-cleaning, low adhesion, and drag reduction. Prog Mater Sci 56:1–108

[3] Cassie ABD, Baxter S (1944) Wettability of porous surfaces. Trans Faraday Soc 40:546–551

[4] Crick CR, Parkin IP (2010) Preparation and characterisation of super-hydrophobic surfaces. Chem Eur J 16:3568–3588

[5] Gao D, Jia M (2015) Hierarchical ZnO particles grafting by fluorocarbon polymer derivative: preparation and superhydrophobic behavior. Appl Surf Sci 343:172–180

[6] Tian ZR, Voigt JA, Liu JUN, Mckenzie B, Mcdermott MJ, Rodriguez MA, Konishi H, Xu H (2003) Complex and oriented ZnO nanostructures. Nature 2:821–826

[7] Zheng J, Song J, Jiang Q, Lian J (2012) Superhydrophobic behavior and optical properties of ZnO film fabricated by hydrothermal method. J Mater Sci Technol 28:103–108

[8] Wu J, Xia J, Lei W, Wang B (2010) Superhydrophobic surface based on a coral-like hierarchical structure of ZnO. PLoS One. 5:e14475

[9] Salek G, Tenailleau C, Dufour P, Guillemet-Fritsch S (2015) Room temperature inorganic polycondensation of oxide (Cu$_2$O and ZnO) nanoparticles and thin films preparation by the dip-coating technique. Thin Solid Films 589:872–876

[10] Sun Y, Wang L, Yu X, Chen K (2012) Facile synthesis of flower-like 3D ZnO superstructures via solution route. Cryst Eng Comm 14:3199–3204

[11] Wu J-J, Liu S-C (2002) Low-temperature growth of well-aligned ZnO nanorods by chemical vapor deposition. Adv Mater 14:215–218

[12] Ennaceri H, Wang L, Erfurt D, Riedel W, Mangalgiri G, Khaldoun A, El Kenz A, Benyoussef A, Ennaoui A (2016) Water-resistant surfaces using zinc oxide structured nanorod arrays with switchable wetting property. Surf Coatings Technol 299:169–176

[13] Guo X, Li X (2017) An expanding horizon: facile fabrication of highly superhydrophobic coatings. Mater Lett 186:357–360

[14] Feng X, Feng L, Jin M, Zhai J, Jiang L, Zhu D (2004) Reversible super-hydrophobicity to super-hydrophilicity transition of aligned ZnO nanorod films. J Am Chem Soc 126:62–63

[15] Zhang D, Wang L, Qian H, Li X (2016) Superhydrophobic surfaces for corrosion protection: a review of recent progresses and future directions. J. Coatings Technol Res 13:11–29

[16] Sue K, Kimura K, Murata K, Arai K (2004) Effect of cations and anions on properties of zinc oxide particles synthesized in supercritical water. J Supercrit Fluids 30:325–331

[17] Anžlovar A, Kogej K, Orel ZC, Žigon M (2014) Impact of inorganic hydroxides on ZnO nanoparticle formation and morphology. Cryst Growth Des 14:4262–4269

[18] Uekawa N, Yamashita R, Jun Wu Y, Kakegawa K (2004) Effect of alkali metal hydroxide on formation processes of zinc oxide crystallites from aqueous solutions containing Zn(OH)$_4^{2-}$ ions. Phys Chem Chem Phys 6:442–446

[19] Rahoui S, Turq V, Bonino J-P (2013) Effect of thermal treatment on mechanical and tribological properties of hybrid coatings deposited by sol–gel route on stainless steel. Surf Coatings Technol 235:15–23

[20] Cambon JB, Ansart F, Bonino JP, Turq V (2012) Effect of cerium concentration on corrosion resistance and polymerization of hybrid sol-gel coating on martensitic stainless steel. Prog Org Coatings 75:486–493

[21] Meiffren V, Dumont K, Lenormand P, Ansart F, Manov S (2011) Development of new processes to protect zinc against corrosion, suitable for on-site use. Prog Org Coatings 71:329–335

[22] Ebert D, Bhushan B (2012) Transparent, superhydrophobic, and wear-resistant coatings on glass and polymer substrates using SiO2, ZnO, and ITO nanoparticles. Langmuir 28:11391–11399

[23] Nishimoto S, Kubo A, Nohara K, Zhang X, Taneichi N, Okui T, Liu Z, Nakata K, Sakai H, Murakami T, Abe M, Komine T, Fujishima A (2009) TiO$_2$-based superhydrophobic-superhydrophilic patterns: fabrication via an ink-jet technique and application in offset printing. Appl Surf Sci 255:6221–6225

[24] Williamson GK, Hall WH (1953) X-ray line broadening from filed aluminium and wolfram. Acta Metall 1:22–31

[25] Mote V, Purushotham Y, Dole B (2012) Williamson-Hall analysis in estimation of lattice strain in nanometer-sized ZnO particles. J Theor Appl. Phys. 6:6

[26] Lujun Y, Maojun Z, Changli L, Li M, Wenzhong S (2012) Facile synthesis of superhydrophobic surface of ZnO nano-flakes: chemical coating and UV-induced wettability conversion. Nanoscale Res Lett 7:216

[27] Nakajima A, Abe K, Hashimoto K, Watanabe T (2000) Preparation of hard super-hydrophobic films with visible light transmission. Thin Solid Films 376:140–143

[28] Li H, Lai Y, Huang J, Tang Y, Yang L, Chen Z, Zhang K (2015) Multifunctional wettability patterns prepared by laser processing on superhydrophobic TiO2 nanostructured surfaces. J Mater Chem B 3:342–347

[29] Li Y, Chen S, Wu M, Sun J (2014) All spraying processes for the fabrication of robust, self-healing, superhydrophobic coatings. Adv Mater 26:3344–3348

[30] Yuan Z, Bin J, Wang M, Huang J, Peng C, Xing S, Xiao J, Zeng J, Xiao X, Fu X (2014) Preparation of a poly-dimethylsiloxane (PDMS)/$CaCO_3$ based superhydrophobic coating. Surf Coat Technol 254:97–103

F-ZnO-Na-FC-E   F-ZnO-Na-FC   F-ZnO-Li-FC-E   F-ZnO-Li-FC

-CH$_2$-

C-H